Quaternary Science Reviews 251 (2021) 106712

Contents lists available at ScienceDirect

Quaternary Science Reviews

journal homepage: www.elsevier.com/locate/quascirev

Tree-ring based minimum temperature reconstruction on the southeastern Tibetan Plateau

Maierdang Keyimu [a], Zongshan Li [a, *], Guohua Liu [a], Bojie Fu [a], Zexin Fan [b], Xiaochun Wang [c], Xiuchen Wu [d], Yuandong Zhang [e], Umut Halik [f]

[a] State Key Laboratory of Urban and Regional Ecology, Research Center for Eco-Environmental Sciences, Chinese Academy of Sciences, Beijing, 100085, China
[b] Xishuangbanna Tropical Botanical Garden, Chinese Academy of Sciences, Mengla, 666303, China
[c] College of Forestry, Northeast Forestry University, Harbin, 150040, China
[d] State Key Laboratory of Earth Surface Processes and Resource Ecology, Beijing Normal University, Beijing, 100875, China
[e] Key Laboratory of Forest Ecology and Environment, State Forestry Administration, Institute of Forest Ecology, Environment and Protection, Chinese Academy of Forestry, Beijing, 100091, China
[f] College of Resource and Environment Sciences, Xinjiang University, Urumqi, 830046, China

ARTICLE INFO

Article history:
Received 10 June 2020
Received in revised form
6 November 2020
Accepted 9 November 2020
Available online 18 November 2020

Keywords:
Paleoclimatology
Tree-rings
Annual minimum temperature
Forcing
Southeastern Tibetan Plateau

ABSTRACT

Increases in the annual minimum temperature (Tmin) has been more obvious than the increase in the annual mean temperature in the southeastern Tibetan Plateau (TP) over the past few decades; however, annual Tmin variability over the long-term in the southeastern TP has received scant attention. Here, we present a 413-year long tree-ring width chronology (TRW), which is composed of 22 site chronologies at high altitudes at the Hengduan Mountains on the southeastern TP. Climate–tree growth relationship analysis revealed that annual Tmin was the climatic factor that influenced radial tree growth in the area the most ($R = 0.74$, $P < 0.001$). Accordingly, we reconstructed the annual Tmin over the 1600–2012 AD period on the southeastern TP. The linear regression model between TRW chronology and annual Tmin accounted for 54.3% of the total variance in actual Tmin during the common period, 1960–2012. The close coupling of warm and cold episodes with other temperature reconstructions from surrounding regions indicated the reliability of our reconstruction. In addition, the comparison of reconstructed series with Climate Research Unit gridded data demonstrated that our reconstruction could represent the large-scale variability in annual Tmin on the TP. Furthermore, the Tmin variability exhibited similar trends with the temperature reconstructions from the TP, Asia, and northern hemisphere during the common period (1600–2012), indicating that the thermal variation in southeastern TP was consistent with the continental and hemispheric scale climate system variabilities. Atlantic Multi-Decadal Oscillation (AMO) and solar activity were observed to be key factors influencing annual Tmin variation over the southeastern TP. The results of the moving correlation analyses implied that the radial forest growth at high altitudes on the southeastern TP remained consistent with regional Tmin variation, and the decrease in precipitation has not yet limited forest growth.

1. Introduction

Tree-rings are widely considered as one of the most reliable sources of past environmental information (Fritts, 1976; Briffa et al., 1998; Esper et al., 2002), and are key proxies for centurial to millennial-scale climatic reconstructions (Esper et al., 2002; Zhang et al., 2003; D'Arrigo et al., 2005; Briffa et al., 2008; Yang et al., 2014). However, concerns have been raised with regard to the capacity of tree-rings to provide reliable climate data, especially temperature variability data, in the wake of warming-induced saturation effects (Reich and Oleksyn, 2008; Williams et al., 2010a), increased drought intensity (Williams et al., 2011; Charney et al., 2016; Babst et al., 2019), and disturbance from agents such as insect pest infestations and fires, which have led to declines in regional forest growth or increased tree mortality (Williams et al., 2010a,b). Conversely, numerous studies have also reported a positive effect of increasing temperatures on forest growth (Liang et al., 2009; Salzer et al., 2009; Dulamsuren et al., 2017; Shi et al.,

* Corresponding author.
E-mail address: zsli_st@rcees.ac.cn (Z. Li).

https://doi.org/10.1016/j.quascirev.2020.106712
0277-3791/

2020). Trees, particularly those growing at high elevations and close to the upper tree line, where temperature is a major factor limiting tree growth, are maintaining growth trends consistent with climate warming (Salzer et al., 2009; Shi et al., 2019a,b), while still portraying historical thermal trends in regions.

The average global surface temperatures have risen by approximately 0.85 °C (0.65–1.06 °C) in the 20th century and are projected to rise by 1.4–4.8 °C in the 21st century (IPCC et al., 2013, under the RCP8.5 scenario). Climate warming has diminished the influence of key climatic factors limiting plant growth, and could increase the net primary productivity (NPP) of terrestrial vegetation (Myneni et al., 1997; Nemani et al., 2003), mainly due to an increase in photosynthetic rates and water use efficiency (Ali et al., 2015; Voelker et al., 2016), in addition to the extension of the active growing season periods (Anav et al., 2015; Zhu et al., 2016). Numerous studies on tree-growth–climate interactions at tree lines, as well as climate reconstructions based on dendrochronology have reported positive growth responses of tree line trees to warmer temperatures (Bräuning, 1994, 2006; Bräuning and Mantwill, 2004; Harsch et al., 2009; Liang et al., 2009; Salzer et al., 2009; Kullman, 2013; Qi et al., 2015; Cao et al., 2018; Shi et al., 2020).

The southeastern Tibetan Plateau (TP) belongs to the so-called subtropical alpine canyon region, with abundant annual rainfall. Available climate records have revealed increasing temperatures in the region over the 1960–2012 period, and the temperature increase has been more dramatic since 1980. Dendroclimatological studies have also revealed that temperature is the major limiting factor for forest growth at high altitudes in the region, with the influence of precipitation being insignificant; therefore, numerous historical temperature reconstruction studies have investigated regional thermal variability over the long term. For example, Fan et al. (2009) and Li et al. (2012) reconstructed the summer mean temperatures for the 1750–2006 and 1475–2003 periods, while Liang et al. (2016b) reconstructed the August mean minimum temperatures in 1630–2011, Zhu et al., 2016 reconstructed the July and August mean maximum temperatures in 1645–2012, Li and Li (2017), and Keyimu et al. (2020) reconstructed the annual mean minimum temperatures for the 1451–2014 and 1837–2017 periods, respectively. In addition, Huang et al. (2019) reconstructed the winter temperature for the 1340–2007 period. However, the studies were conducted only in a few sampling sites. In addition, based on the instrumental temperature data on the southeastern TP, the rise in annual minimum temperature (R = 0.87, slope = 0.29 °C/decade) was more rapid than the rise in the annual mean temperature (R = 0.77, slope = 0.21 °C/decade). However, the long-term variability in annual minimum temperature in the region has hardly received any attention. The reconstruction of historical minimum temperatures could enrich the understanding of regional thermal variation from a long-term perspective and current warming trends, in addition to forest growth responses to such warming trends.

The objectives of the present study were to (1) develop a TRW chronology in the southeastern TP using a tree-ring network, (2) determine the key climatic factors influencing radial tree growth, (3) reconstruct thermal variability over the long term context, (4) compare thermal variability across different temperature reconstruction records, and (5) investigate if forest growth rate trends are correlated with recent climate change trends on the southeastern TP.

2. Study area

The southeastern TP (Fig. 1) extends across Xizang, Yunnan, and Sichuan provinces in China, with the elevation ranging from 100 m to 7000 m. The climate of the area is under the influence of the westerly and monsoon circulations of the Indian and Pacific Oceans, with pronounced dry and wet seasonality (Liang et al., 2008, 2009; Li et al., 2012; Huang et al., 2019; Keyimu et al., 2020). According to the climate data (time span 1960–2012) from meteorological stations near to tree-ring sampling sites, the multi-years annual total precipitation was 754 mm, more than 70% of the precipitation was concentrated during May–September. The monthly average maximum, mean, and minimum temperatures were 15.8 °C, 7.9 °C, 2.3 °C, respectively (Fig. 2). The relatively steep topography at high altitudes in southeastern TP is not favorable for soil development; therefore, a thin soil layer consisting mainly of dark-brown earths, alpine meadow soil, and burozem soil (Chinese Soil Taxonomy) cover the bedrock. The typical subalpine coniferous forests grow at high elevations in the southeastern TP, and the major tree genera are *Abies*, *Larix*, *Tsuga*, *Pinus*, and *Sabina*.

3. Materials and methods

3.1. Tree-ring dataset

We collected TRW measurements at 98 sites on the southeastern TP from dominant species in subalpine coniferous forests. Out of the 98 sites, 72 sites are datasets from the present study, while the remaining 26 sites were obtained from the International Tree Ring Data Bank (https://www.ncdc.noaa.gov/data-access/paleoclimatology data/datasets/tree-ring). We detrended the raw tree-ring data from each site to remove the age related biological trend of tree growth using a negative exponential model (Cook and Kairiukstis, 1990; Li et al., 2012; Liang et al., 2016b; Huang et al., 2019). Tukey's biweight robust mean method was applied to average the dimensionless tree-ring width indices to achieve standard chronology. Twenty-two chronologies (Fig. 1, Fig. S1a, S1b; Table S1) in the available dataset were selected as temperature sensitive based on their correlation with monthly temperature records from the nearest meteorological stations (Fig. S2a, 2b). The correlation analysis among temperature sensitive chronologies revealed the similarities among the 22 chronologies (the average correlation index was 0.29, $P < 0.01$) (Table S2), indicating correlated tree radial growth at the sites. The Express Population Signal (EPS) values of 12 chronologies were higher than the 0.85 threshold value (Wigley et al., 1984), while the EPS values of 10 chronologies were lower than 0.85 at the earlier years, although they included at least six sample replicates. The final chronology dataset included the four coniferous genera, including *Abies*, *Picea*, *Sabina*, and *Pinus*. At the end, the 22 TRW chronologies were averaged into one chronology and used for further analyses.

3.2. Climate data

Monthly maximum, minimum, mean temperature, and precipitation climate data were obtained from 11 Chinese national meteorological stations, which were close to each tree ring sampling site (Fig. 1). Climate data from weather stations vary across the region; therefore, we selected a common data interval, 1960 to 2012, and averaged the data into single temperature and precipitation series to perform tree growth–climate relationship analyses.

3.3. Data analysis

To determine the key climatic factors influencing radial tree growth, we conducted growth–climate correlation analyses between TRW chronology and climate variables (maximum temperature, minimum temperature, mean temperature, and

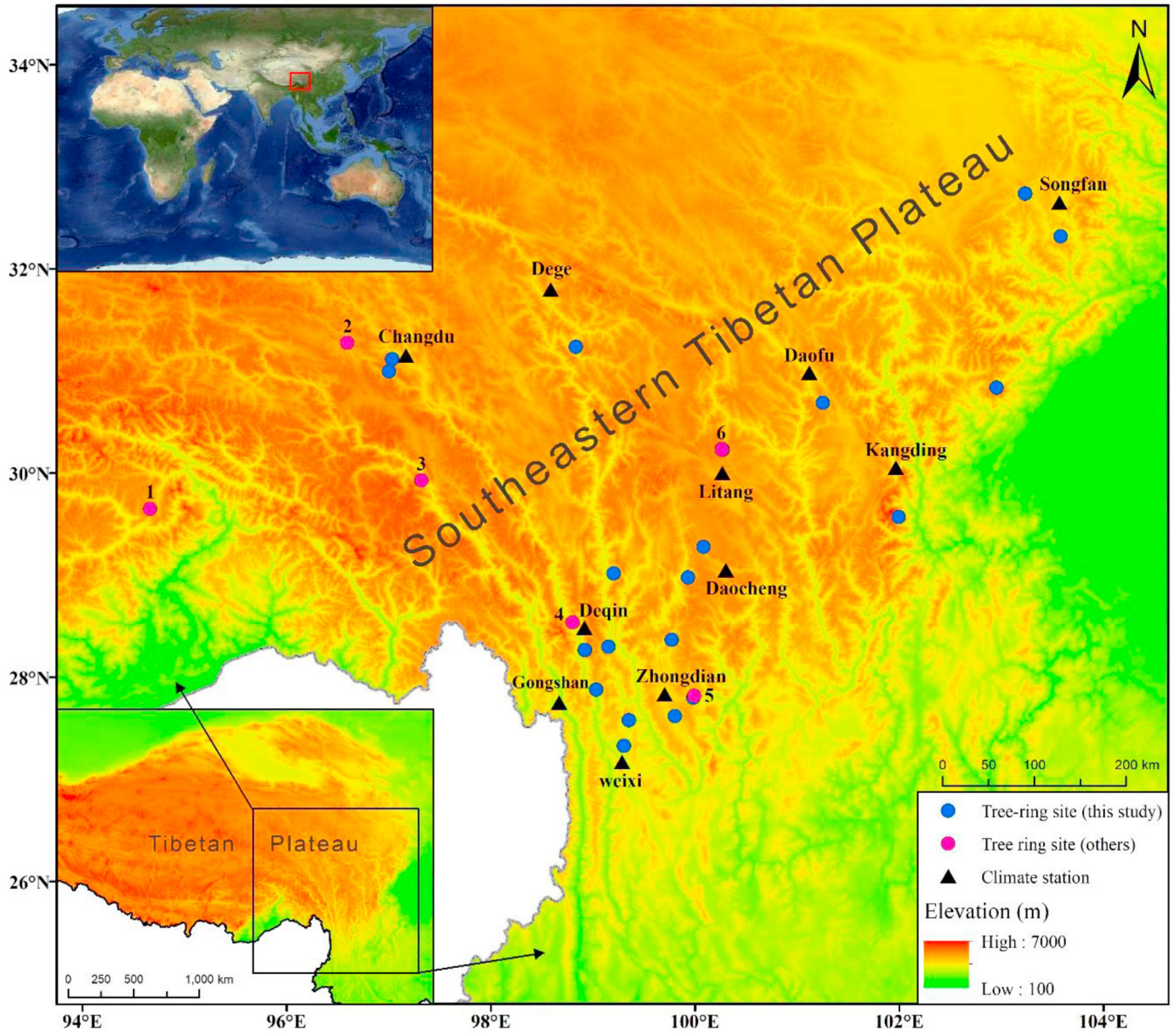

Fig. 1. Tree-ring sampling sites in the southeastern Tibetan Plateau. Blue dots represent the 22 tree-ring sites explored within the present study, pink dots represent study sites of other studies (from 1 to 6 are Fan et al., 2009; Liang et al., 2009; Li et al., 2012; Liang et al., 2016a; Li and Li, 2017; Huang et al., 2019, respectively). Black triangles represent meteorological stations in Changdu, Dege, Deqin, Gongshan, Weixi, Zhongdian, Daocheng, Litang, Kangding, Daofu, and Songfan Counties. (For interpretation of the references to color in this figure legend, the reader is referred to the Web version of this article.)

precipitation) adopting the correlation and response function analyses using Dendroclim 2002 software (Biondi and Waikul, 2004) for the 1960–2012 period. Considering that tree growth is not only influenced by climatic conditions during current year, but also from previous year (legacy effect) (Fritts, 1976), our climate – tree growth relationship analysis included the monthly windows from previous year June until current year November. We also tried seasonal aggregation (annual, spring, summer, autumn, and winter) of climate data since averaged climate variables can make more eco-physiological sense than just one single month. A moving correlation analysis between TRW chronology and annual mean minimum temperature was conducted at 32-year intervals to investigate the temporal variability of the correlation between radial tree growth and limiting factor. Moving correlation analysis was also conducted between TRW chronology and precipitation to investigate the dynamic influences of precipitation on forest growth, and whether water stress influenced forest growth.

4. Results

4.1. Climate–tree growth response analysis

Results of correlation and response function analyses between the average TRW chronology and monthly average, annual and seasonal aggregated climate records were demonstrated in Fig. 3. According to the results, the correlation between TRW chronology and Tmin was stronger than the correlation between Tmax and Tmean (over the 1960–2012 common period). The correlation between Tmin and chronology was significant at the 99% confidence level throughout all the investigated periods except for previous

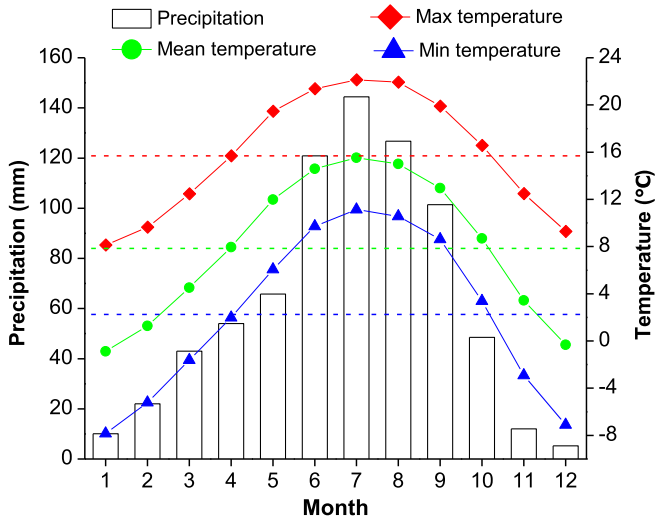

Fig. 2. Ombrothermic diagram of climate variables in the southeastern Tibetan Plateau. Monthly total precipitation (bars), mean maximum temperature (red line with squares), mean temperature (green line with circles), and mean minimum temperature (blue line with triangles), calculated using the available climate data from meteorological stations in Changdu, Dege, Deqin, Gongshan, Weixi, Zhongdian, Daocheng, Litang, Kangding, Daofu, and Songfan Counties. Horizontal dashed red, green, and blue lines represent the average of maximum, mean, and minimum temperatures, respectively. (For interpretation of the references to color in this figure legend, the reader is referred to the Web version of this article.)

year July (but significant at 95%). The correlation between chronology and monthly average and seasonalized precipitation was positive in 17 out of 23 investigation windows, but the significant correlation (at 95% level) only occurred in May and spring of current year. The correlation between TRW chronology and annual Tmin was found to be highest ($R = 0.74$, $P < 0.01$). In addition, the result of the climate response function analysis between chronology and annual Tmin was significant. Therefore, we used the annual Tmin to reconstruct in present study.

4.2. Annual Tmin reconstruction and its validation

We reconstructed historical (1600–2012 A.D.) annual Tmin (Fig. 4) based on the relationship between average TRW chronology and instrumental annual Tmin. The climate reconstruction data are listed in Table S3, and the results indicated that the reconstructions were reliable. The reconstruction explained 54.3% of the variability in Tmin. The thermal variability observed in our newly reconstructed temperature series not only matched other temperature reconstructions from surrounding sites (Fig. 5), but also the long-term thermal variability in the TP, Asia, and the northern hemisphere (Fig. 6). Spatial correlation analyses between the reconstructed series and Climate Research Unit (CRU) gridded data revealed that our reconstruction could capture the broad-scale thermal variability on the southeastern TP as well as the entire TP (Fig. 7). According to the results of the multi-taper-spectrum analysis, there were short (2–3 years) and long cycles (24.2 and 54.9 years) of Tmin variability in the 413-year reconstruction (Fig. 8). Warm/cold episodes in the reconstruction were coupled with warm/cold phases of Atlantic Multi-decadal Oscillation (AMO) and strong/weak solar irradiance (Fig. 9), implying that the AMO and solar activity exerted considerable influence on the thermal variability in the southeastern TP. Based on the reconstructed series, the annual Tmin increased markedly after the 1980s, and such an increase was unprecedented over the long-term on the southeastern TP.

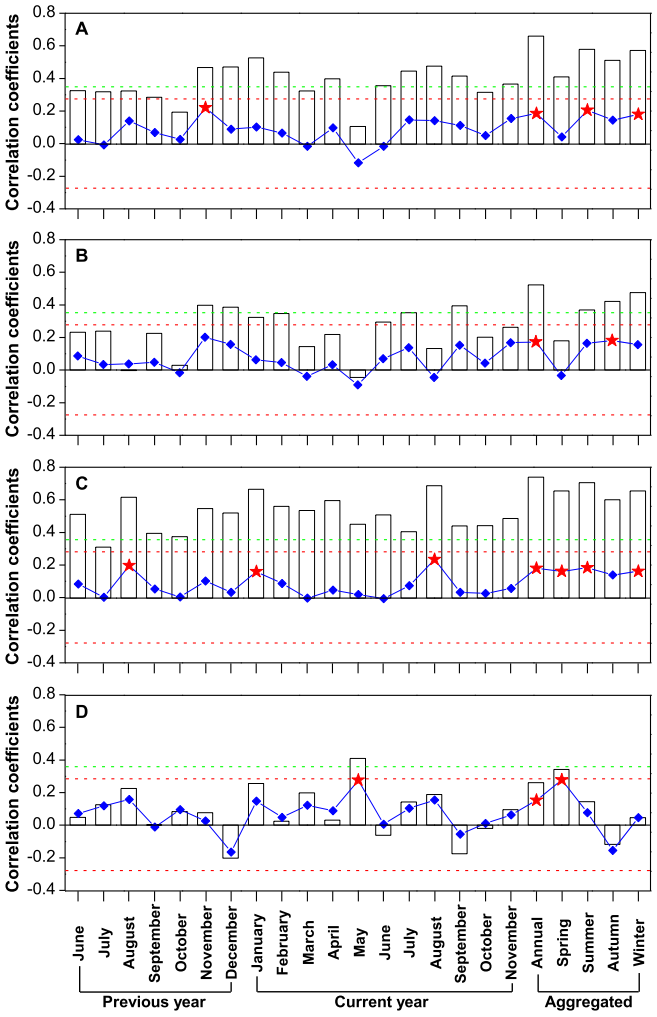

Fig. 3. Results of correlation and response function analyses between TRW chronology and monthly mean (A), maximum (B), minimum temperatures (C), and precipitation (D). The bar graphs denote the results of correlation analysis. The line graphs denote the results of response function analysis. The horizontal red and green dashed lines denote the 0.05 and 0.01 significant levels of correlation, respectively. The red stars on the lines denote the significant effects ($p < 0.05$) of response function analysis. (For interpretation of the references to color in this figure legend, the reader is referred to the Web version of this article.)

Radial tree growth accelerated drastically with increases in temperatures since 1980s, and the levels of increase were unprecedented over the previous 413 years. Correlation result demonstrated the close association between regional TRW chronology and Tmin variation ($R = 0.74$, $P < 0.01$). In addition, the moving correlation results between the chronology and Tmin were significant (>95% confidence level) during most of the investigated period (1960–2012) (Fig. 10), indicating that radial tree growth is maintaining a correlation with annual Tmin on the southeastern TP, and that a divergence between forest growth and Tmin variation has not occurred.

5. Discussion

5.1. Climate – radial tree growth relationship

Based on the correlation between TRW chronology and climate variables, the annual Tmin was the key climatic factor influencing radial tree growth in conifer species at higher elevations on the

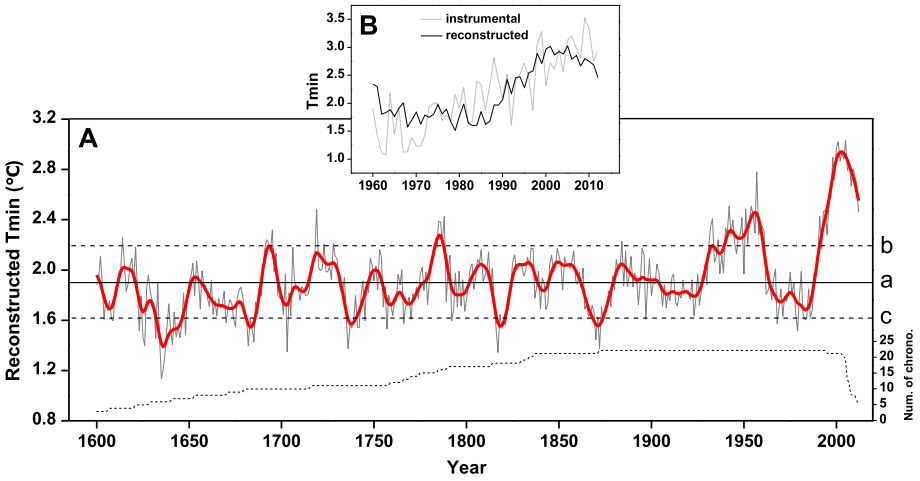

Fig. 4. A: Tree-ring based annual Tmin reconstruction in the southeastern Tibetan Plateau (grey thin line denotes the raw reconstruction series, and the red bold line denotes the 11-year loess smoothing results of the reconstruction). The horizontal black line (a) represents the mean value of reconstruction, the upper (b) and lower (c) horizontal dashed lines represent the standard deviation value. The dashed black line at the bottom is the number of chronology corresponding with the reconstruction series. **B**: The comparison of instrumental (grey line) and reconstructed (black line) annual Tmin during the common period 1960–2012. (For interpretation of the references to color in this figure legend, the reader is referred to the Web version of this article.)

southeastern TP. Tmin influences the division and enlargement of conifer tracheids during the growth season (Deslauriers et al., 2008). In addition, according to Hosoo et al. (2002), xylem lignification mainly takes place at night, implying the significance of Tmin, which is often observed during the night, for radial tree growth. Conversely, higher spring and autumn temperatures extend the growth season (Menzel et al., 2006; Piao et al., 2007), which means an early onset of cambium activity and xylem cell production as well as a longer duration of xylem formation (Huang et al., 2011; Boulouf-Lugo et al., 2012), which, in turn, leads to wider tree-rings.

Climate factors often exert time-lag effects on tree growth (Fritts, 1976). The results of tree growth–climate relationship analyses in the present study also revealed considerable time-lag effects of the previous year Tmin on the radial tree growth of the subsequent year. The extension of the growth season (late growth season) prolongs the period of photosynthetic activity due to the lengthened photoperiod (Jackson, 2009), which enables the storage of more carbohydrates in parenchyma tissues, and such carbohydrates could be used in the spring of the growth season of the following year (McMahon et al., 2011), when the photosynthetic activity is still low, which supports the strong legacy effect of previous year climate factors on tree growth in the subsequent year in our study.

As indicated by the tree growth–climate relationship analyses results, winter Tmin exerted significant influence on the radial tree growth, which can be attributed to the higher Tmin during winter potentially reducing the damage exerted by cold stress on bud and root systems, in addition to prolonging the duration of needle retention in conifers (Pederson et al., 2004; Körner, 2012). Our results also showed a significant positive influence of spring (February–March–April) Tmin on radial tree growth, potentially because the higher Tmin during spring may accelerate the melting of soil frost layer and, in turn, increase water availability, which benefits tree growth. In addition, higher Tmin in spring could advance the onset of cambium layer activity, and, in turn, facilitate tree growth (Williams et al., 2015). A significant influence of the precipitation during current year's May and spring on radial tree growth was also observed (Fig. 3), which highlighted the importance of moisture availability on tree growth during spring, when the cambium layer is most active in the year (Schweingruber, 2007). However, the influence of spring precipitation on radial tree growth has weakened and was below the significant level over the past decade as demonstrated by moving correlation analysis (Fig. S6).

5.2. Comparison with other reconstructions

To validate the reliability of the new Tmin reconstruction series on the southeastern TP, it was compared with other temperature reconstructions of previous studies from surrounding sites, including annual Tmin reconstruction by Li and Li (2017), August Tmin reconstruction by Liang et al. (2016b), winter Tmean reconstruction by Huang et al. (2019), summer Tmean reconstruction by Fan et al. (2009), summer Tmean reconstruction by Li et al. (2012), and summer Tmean reconstruction by Liang et al. (2009), during their common period. We applied 11-year loess smoothing on each of the reconstruction series to increase the visibility of the comparisons. The graphical comparisons displayed the similarities of warm/cold episodes under different reconstructions (Fig. 5). As illustrated in Fig. 5, the 1630s–1640s (except in Fan et al., 2009; Liang et al., 2009), 1760s–1770s, 1810s–1820s, 1910–1920s, and 1970s–1980s intervals had notable cold episodes, while the 1720s–1730s (except in Liang et al., 2009 and Fan et al., 2009), 1770s–1880s, and 1940s–1960s, had warm episodes, and the 2000s had the unprecedented warm years under all reconstructions in southeastern TP over the past four centuries. Nevertheless, there were some discrepancies among the different reconstruction series, which could be attributed to the heterogeneous microclimate environments among the investigated sites, different targets of reconstruction (month/seasons), use of different types of tree-ring proxies (width/density), inconsistent variability in Tmax/Tmean/Tmin (Wilson and Luckman, 2002, 2003), different timespans of available instrumental climate records for calibrating the tree-ring data, sample replications (Esper et al., 2016), application of different methods to detrend the tree-ring data (Huang et al., 2019), in addition to diverse genetic and morphological characteristics among tree species.

The spatial correlation analysis between the reconstructed Tmin and CRU gridded data (TS 4.03) revealed that the new reconstruction could represent the annual Tmin variability of the investigated region as well as the entire TP (Fig. 7). Notably, the spatial

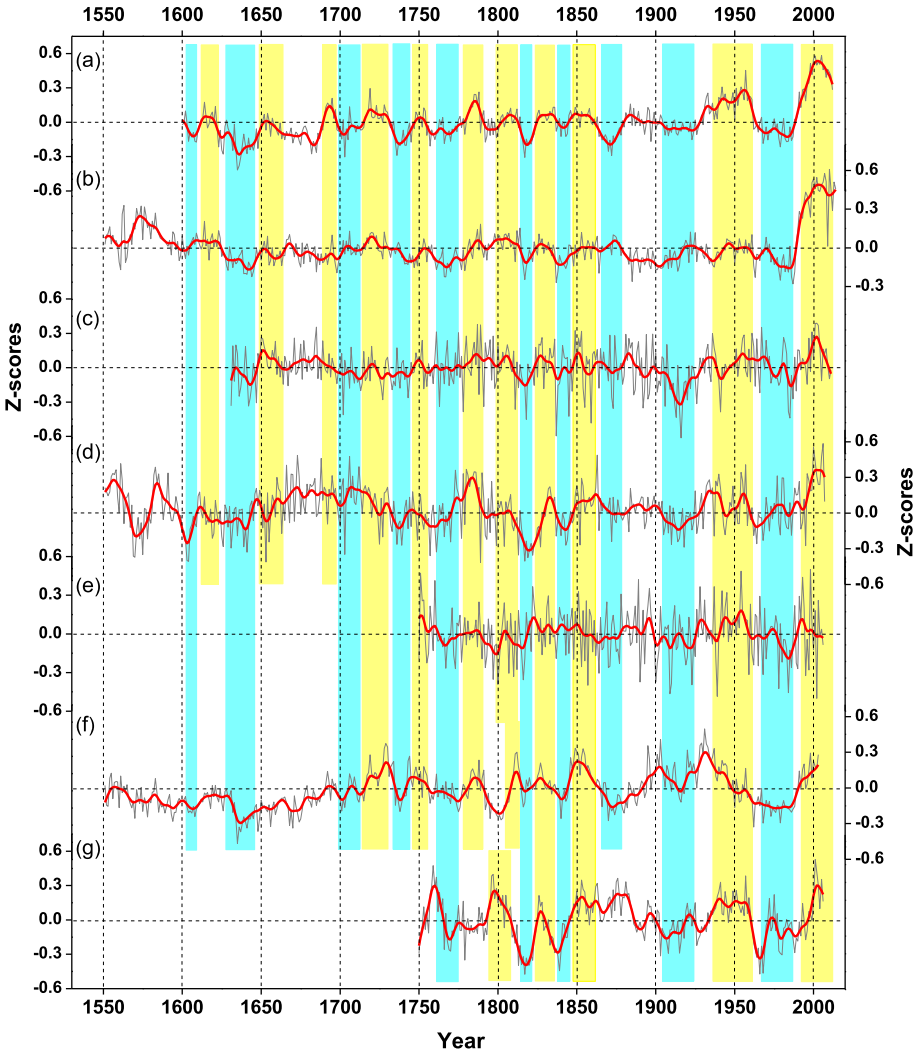

Fig. 5. Comparison of annual Tmin reconstruction with other temperature records on the southeastern Tibetan Plateau. (a) Annual Tmin reconstruction in present study, (b) Annual Tmin reconstruction on the east central TP (Li and Li, 2017), (c) August Tmin reconstruction on the southeastern TP (Liang et al., 2016b), (d) Winter Tmin reconstruction on the southeastern TP (Huang et al., 2019), (e) April–September Tmean reconstruction on the southeastern TP (Fan et al., 2009), (f) Summer Tmean reconstruction on the southeastern TP (Li et al., 2012), (g) Summer Tmean reconstruction on the southeast TP (Liang et al., 2009). All series were Z-scored for direct comparison. Thin grey line in each panel denotes raw reconstruction series, the red bold line denotes an 11-year loess smoothing. Yellow and cyan vertical shadings represent the warm and cold episodes, respectively. (For interpretation of the references to color in this figure legend, the reader is referred to the Web version of this article.)

correlation analyses in the southeastern TP revealed lower and heterogeneous spatial correlation in comparison to those in the other parts of TP, implying variability of climate system, which could be due to the complex terrain, high mountain ranges with deep-cut gorges, and steep topography across the southeastern TP (Fan et al., 2009).

We further compared our Tmin reconstruction series with the summer Tmin reconstruction of the entire TP (Shi et al., 2019b), Asia Tmin reconstruction (PAGES 2k Consortium, 2013), and northern hemisphere (NH) temperature reconstructions by Mann et al. (2009), D'Arrigo et al. (2006), Wilson et al. (2016), Stoffel et al. (2015), and Schneider et al. (2015) over their common periods, including 1648–2005, 1600–1989, 1600–2006, 1600–1995, 1600–2002, 1600–2002, and 1600–2002, respectively. The correlation coefficients between the raw data series (Fig. S3) and the 30-year splined data series (Fig. 6) for the annual Tmin in the southeastern TP in the present, summer Tmin of TP (Shi et al., 2019b), annual Tmin of Asia (PAGES 2k Consortium, 2013), and four different northern hemisphere temperature data (in sequence: Mann et al., 2009; D'Arrigo et al., 2006; Wilson et al., 2016; Stoffel et al., 2015; Schneider et al., 2015) during their common periods were 0.69, 0.27, 0.54, 0.30, 0.35, 0.30, and 0.27, and 0.79, 0.37, 0.73, 0.53, 0.55, 0.64 and, 0.64, respectively (all significant at 99% confidence level), demonstrating the close correlation between the regional Tmin variation in southeastern TP with continental and hemispheric thermal variation at both interannual and multi-decadal time scales. According to the regional, continental, and hemispheric level reconstructions, 1940s–1960s were warm periods, and the warming since late 20th century was unprecedented. Discrepancies were observed among the reconstructions; for instance, Asia and northern hemisphere were cold during the early 19th century, but the southeastern TP was comparatively warm during the period. Nevertheless, the varying patterns of Tmin in the southeastern TP recorded over the past four centuries were synchronous with continental and hemispheric thermal variation on the whole, indicating that the thermo-dynamics of the southern TP are part of a large-scale climate system.

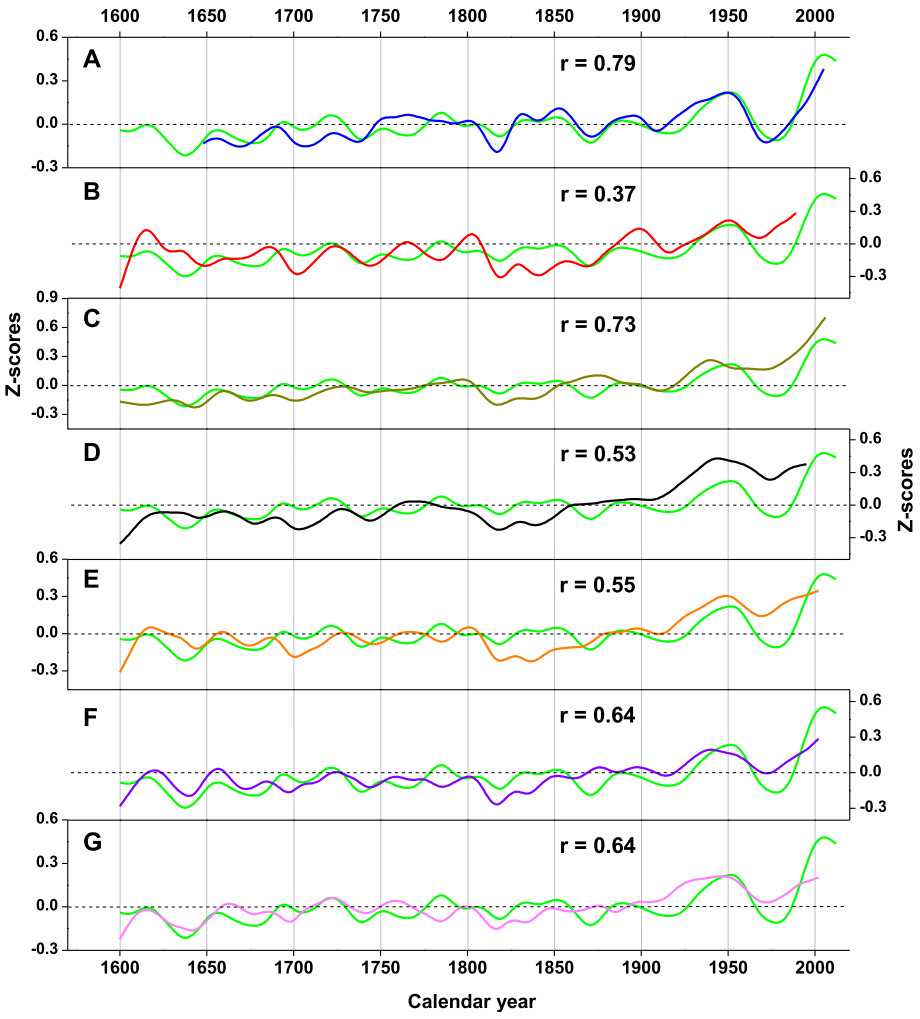

Fig. 6. Panel **A**: Comparison of reconstructed annual Tmin record with summer Tmin record of Tibetan Plateau (Shi et al., 2019b), Panel **B**: Asia Tmin (PAGES 2k Consortium, 2013), Panel **C**: Northern Hemisphere (Mann et al., 2009), Panel **D**: Northern Hemisphere (D'Arrigo et al., 2006), Panel **E**: Northern Hemisphere (Wilson et al., 2016), Panel **F**: Northern Hemisphere (Stoffel et al., 2015), Panel **G**: Northern Hemisphere (Schneider et al., 2015). All series were Z-score normalized and 30-year loess smoothed, and then correlations were evaluated.

5.3. Potential external factors influencing temperature variability

Short and long-term variabilities were observed in our Tmin records. Dendroclimatological studies on the TP suggested a linkage between thermal variability at short and long-term variability with extensive atmospheric–sea surface interactions, such as El Nino Southern Oscillation (ENSO), AMO, Pacific Decadal Oscillation (PDO), and Indian monsoon activity (He et al., 2014; Wang et al., 2014, 2015, 2017a; Li and Li, 2017; Shi et al., 2017, 2019b). We carried out correlation analyses between reconstructed annual Tmin records in the present study and the ENSO reconstruction by Li et al. (2011), PDO reconstruction by MacDonald and Case (2005), and the AMO reconstruction by Mann et al. (2009), and the correlation coefficients were 0.004 ($P > 0.1$), 0.11 ($P < 0.05$), and 0.61 ($P < 0.001$), respectively, suggesting that AMO variation was the key factor influencing thermal variability over the southeastern TP. Fig. 9 illustrates the correlation between positive/negative temperature anomalies and warm/cold AMO phases.

Another potential factor influencing thermal variability is solar activity (Gray et al., 2010; Duan and Zhang, 2014). One of the obvious trends of solar activity is the intensification of sunspots. The temperatures at sunspot regions are lower in comparison to the temperatures at the surrounding regions of the surface of the sun; therefore, sunspots appear darker than other regions. When sunspots are intensified, the energy output of the sun increases slightly, which influences the temperature of the earth's atmosphere. As illustrated in Fig. 9, the cold periods of 1620s–1710s and 1790s–1820s coincided with the Maunder and Dalton minima of solar activity, and the warm periods around the 1930s–1960s coincided with the Modern maxima of solar activities. In addition, we conducted correlation analyses between the reconstructed annual Tmin series and annual total sunspot numbers (http://climexp.knmi.nl/getindices.cgi?WMO=SIDCData/sunspots&STATION=sunspots) to investigate the influence of solar activity on the warm/cold trends in our study area. The correlation coefficient between the 25-year moving average Tmin reconstruction series and sunspot numbers (common period 1761–2000) was 0.38 ($P < 0.001$). The results of the analysis above supported the potential linkage between solar activity and thermal variation across the southeastern TP.

5.4. Accelerating forest growth and role of warming climate

Our regional TRW chronology showed that forest growth accelerated on the southeastern TP after the 1980s, and the increase in growth was almost linear, the growth rate around 2000 was

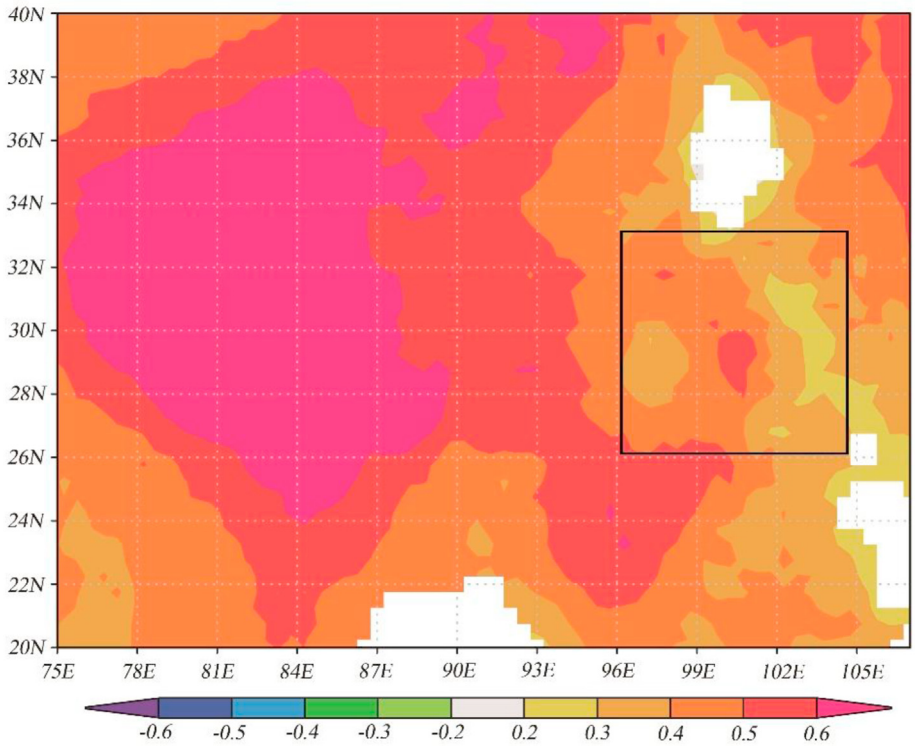

Fig. 7. Spatial correlations of the reconstructed annual Tmin on the southeastern TP from the CRU TS 4.03 dataset for 1901–2012. The analyses were performed using the KNMI climate explorer (Royal Netherlands Meteorological; http://climexp.knmi.nl). The gridded climate dataset was developed by the Climatic Research Unit (Mitchell and Jones, 2005; CRU TS4.03). Black rectangle represents the investigation area within present study. The color key at the bottom represents the correlation coefficient. (For interpretation of the references to color in this figure legend, the reader is referred to the Web version of this article.)

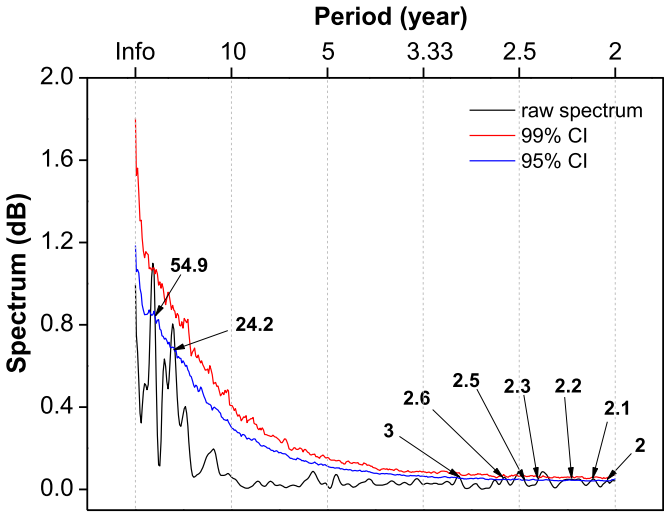

Fig. 8. Multi-taper spectrum analysis of the reconstructed annual Tmin. Blue and red lines denote the 95% and 99% confidence levels (CI confidence intervals), respectively. Significant periods at the 95% confidence level are marked. (For interpretation of the references to color in this figure legend, the reader is referred to the Web version of this article.)

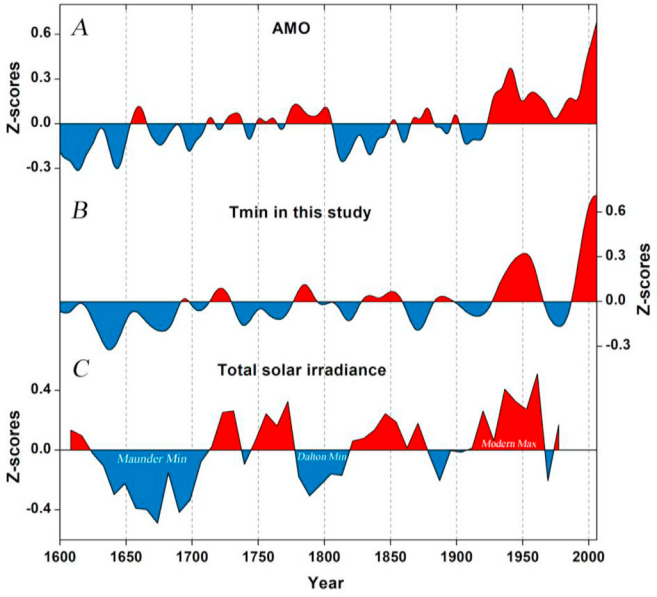

Fig. 9. Comparison of reconstructed annual Tmin in the southeastern TP (**B**) with Atlantic Multi-Decadal Oscillation (Mann et al., 2009) (**A**), and the total solar irradiance (Delaygue and Bard, 2011) (**C**). All series were Z-score normalized for direct comparison. Series **A** and **B** were 30-year Loess smoothed. The blue and red areas represent the cold and warm phases, respectively. (For interpretation of the references to color in this figure legend, the reader is referred to the Web version of this article.)

unprecedented over the past four centuries. The higher correlation between TRW chronology and Tmin suggested the close association between warming climate and accelerating tree growth in the study area. Recent climatic warming has accelerated forest growth in many regions globally, especially at northern altitudes and higher elevations (Salzer et al., 2009; Qi et al., 2015; Dulamsuren et al., 2017; Cao et al., 2019; Shi et al., 2020). The climate warming-induced acceleration of forest growth has also been reported in remote sensing studies. The increase in landscape greenness or Normalized Difference Vegetation Index (NDVI),

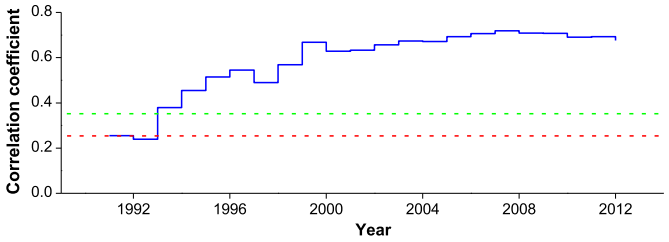

Fig. 10. Results of moving correlation analysis between TRW chronology and annual Tmin (using 32 years moving interval). The dotted red and green lines denote 95% and 99% confidence interval, respectively. (For interpretation of the references to color in this figure legend, the reader is referred to the Web version of this article.)

particularly at northern altitudes and at mountain sites, as well as at high elevations, could imply the acceleration of forest growth. According to Myneni et al. (1997), warming temperatures promoted increases in plant growth at northern high altitude regions following a comparison of 10-year (1981–1991) NDVI data, which were obtained from satellite images of the northern hemisphere. There is also remote sensing evidence that supports our findings of accelerated forest growth on the southeastern TP that have been observed in present study. Wang et al. (2017b) investigated the NPP variation on the Hengduan Mountains by using the NPP statistics of MODIS C6 product, and analyzed the temporal and spatial variation characteristics of NPP. They reported a sustained 10-year (2004–2014) NPP increase in the Hengduan Mountains, and such increase was more obvious at mid and high elevation regions, where mainly consist of coniferous forests.

The positive relationship between regional TRW chronology and temperature in the present study suggested that the rising temperatures facilitate accelerated forest growth at high altitudes in the southeastern TP. Numerous studies have reported the extension of vegetation growth periods globally due to increased temperatures (Keeling et al., 1996; Chen et al., 2005; Jeong et al., 2011). According to Guo et al. (2019) the length of the growth season for coniferous forests in the Hengduan Mountains was extended by 6.4 days over a 10-year period, this may have facilitated tree growth acceleration in the region by prolonging photosynthetic activity/carbohydrate accumulation/lignification periods. In addition, the increase in spring Tmin (Fig. S4) could have eased the temperature constraint on the onset of cambial activity in conifer species on the Hengduan Mountains. Woody species require a threshold temperature to initiate stem cambial activity (Ryan, 2010; Way and Oren, 2010), and only temperature above the threshold could stimulate the inactivated cambium layer cells (Deslauriers et al., 2008; Begum et al., 2010). Although we have no experimental data demonstrating the advance of cambial activity and its potential connection with increasing spring temperature in the present study, we can assume that an increase in spring temperature contributes to the earlier termination of cambial dormancy in spring, and in turn, more rapid tree growth.

The South Asian summer monsoon (SASM) is the source of moisture for the southeastern TP. However, weakening of SASM over the past couple of decades has been reported (Sano et al., 2012; Roxy et al., 2015; Pumijumnong et al., 2020). Instrumental precipitation records have showed decreasing regional precipitation from the 2000s (Fig. S5), which might exert hydrological stress on forest growth in the region, and lead to drought-induced forest growth decline as reported in many other investigations in alpine tree line ecotones (Allen et al., 2010; Peng et al., 2011; Liang et al., 2016a) and mid-latitude mountains. To investigate whether drought stress increased and hindered forest growth, we conducted moving correlation analyses between the precipitations of spring and the monsoon period, and TRW chronology (Fig. S6). According to the results, the influence of the precipitation during the spring and monsoon period showed decrease since the 2000s, indicating that the decreasing precipitation had not yet began to limit forest growth. Therefore, we confirmed that Tmin remained as the primary factor influencing radial tree growth at higher altitudes on the southeastern TP. However, under decreasing precipitation and increasing temperature scenarios on the southeastern TP, precipitation could become a factor limiting radial tree growth and hindering forest growth in future.

6. Conclusion

In present study, we synthesized a regional tree-ring width chronology using 22 site chronologies each was sensitive to annual minimum temperature on the southeastern TP. Based on the tree growth – climate relationship analyses, we developed a transfer model and reconstructed the annual minimum temperature for the past four centuries (A.D. 1600–2012). The results of leave-one-out verification and similarities between present reconstruction series and previous reported historical temperature records indicated the fidelity of the new reconstruction. Based on the consistency of our annual minimum temperature with other historical temperature from the TP, Asia, and northern hemisphere we confirmed that the thermal conditions on the southeastern TP was part of large scale climate systems. Association between the reconstructed annual minimum temperature and total solar irradiance and AMO series implied that the solar and Atlantic Ocean activities were drivers of decadal and multi-decadal thermal variations on the southeastern TP. According to our results, radial growth of high altitude forests in the study area was keeping pace with the rising annual minimum temperature. However, continuously rising temperature and decreasing precipitation might induce drought stress on the forest growth in future. Further investigations are required to carry out modelling works over when coniferous trees at high altitudes in the southeastern TP will become hydraulically stressed.

Author statement

Maierdang Keyimu: Writing - original draft, Conceptualization, Formal analysis, Visualization. Zongshan Li: Investigation, Supervision, Writing - review & editing, Validation. Guohua Liu: Resources, Review & Editing, Validation, Bojie Fu: Resources, Supervision, Review & Editing, Validation, Zexin Fan: Investigation, Data curation, Validation, Xiaochun Wang: Investigation, Data curation, Validation, Xiuchen Wu: Data curation, Validation, Yuandong Zhang: Investigation, Data curation, Validation, Umut Halik: Editing, Validation.

Declaration of competing interest

All the authors listed have approved the revised manuscript, and declared no conflict of interest.

Acknowledgment

This work was funded by the National Key Research Development Program of China (2016YFC0502105), the second Tibetan Plateau Scientific Expedition and Research (STEP) Program (2019QZKK0502) and National Natural Science Foundation of China (NSFC, 31770533). We would like to thank the International Tree-ring Data Bank and those who helped during the fieldwork. We also would like to express our gratitude to the anonymous reviewers for providing us with helpful comments and suggestions to

improve our work.

Appendix A. Supplementary data

Supplementary data to this article can be found online at https://doi.org/10.1016/j.quascirev.2020.106712.

References

Allen, C.D., Macalady, A.K., Chenchouni, H., Bachelet, D., McDowell, N., Vennetier, M., Kitzberger, T., Rigling, A., Breshears, D.D., Hogg, E.H., Gonzalez, P., Fensham, R., Zhang, Z., Castro, J., Demidova, N., Lim, J.H., Allard, G., Running, S.W., Semerci, A., Cobb, N., 2010. A global overview of drought and heat-induced tree mortality reveals emerging climate change risks for forests. For. Ecol. Manag. 259, 660–684. https://doi.org/10.1016/j.foreco.2009.09.001.

Ali, A.A., Xu, C., Rogers, A., Mcdowell, N.G., Medlyn, B.E., Fisher, R.A., Wullschleger, S.D., Reich, P.B., Vrugt, J.A., Bauerle, W.L., Santiago, L.S., Wilson, C.J., 2015. Global scale environmental control of plant photosynthetic capacity. Ecol. Appl. 25 (8), 2349–2365. https://doi.org/10.1890/14-2111.1.

Anav, A., Friedlingstein, P., Beer, C., Ciais, P., Harper, A., Jones, C., Murray-Tortarolo, G., Papale, D., Parazoo, N.C., Peylin, P., Piao, S.L., Sitch, S., Viovy, N., Wiltshire, A., Zhao, M.S., 2015. Spatiotemporal patterns of terrestrial gross primary production: a review. Rev. Geophys. 53 (3), 785–818. https://doi.org/10.1002/2015RG000483.

Babst, F., Bouriaud, O., Poulter, B., Trouet, V., Girardin, M., Frank, D.C., 2019. Twentieth century redistribution in climatic drivers of global tree growth. Sci. Adv. 5, eaat4313. https://doi.org/10.1126/sciadv.aat4313.

Boulouf-Lugo, J., Deslauriers, A., Rossi, S., 2012. Duration of xylogenesis in black spruce lengthened between 1950 and 2010. Ann. Bot. 110, 1099–1108. https://doi.org/10.1093/aob/mcs175.

Begum, S., Nakaba, S., Oribe, Y., Kubo, T., Funada, R., 2010. Cambial sensitivity to rising temperatures by natural condition and artificial heating from late winter to early spring in the evergreen conifer *Cryptomeria japonica*. Trees (Berl.) 24 (1), 43–52. https://doi.org/10.1007/s00468-009-0377-1.

Biondi, F., Waikul, K., 2004. DENDROCLIM2002: a C++ program for statistical calibration of climate signals in tree-ring chronologies. Comput. Geosci. 30 (3), 303–311. https://doi.org/10.1016/j.cageo.2003.11.004.

Bräuning, A., 1994. Dendrochronology for the last 1400 years in eastern Tibet. Geol. J. 34 (1), 75–95.

Bräuning, A., Mantwill, B., 2004. Increase of Indian summer monsoon rainfall on the Tibetan Plateau recorded by tree rings. Geophys. Res. Lett. 31, L24205. https://doi:10.1029/2004GL020793.

Bräuning, A., 2006. Tree-ring evidence of "little ice age" glacier advances in southern tibet. Holocene 16 (3), 369–380. https://doi.org/10.1191/0959683606hl922rp.

Briffa, K.R., Jones, P.D., Schweingruber, F.H., Osborn, T.J., 1998. Influence of volcanic eruptions on Northern Hemisphere summer temperature over the past 600 years. Nature 393 (6684), 450–455. https://doi.org/10.1038/30943.

Briffa, K.R., Shishov, V.V., Melvin, T.M., Vaganov, E.A., Grudd, H., Hantemirov, R.M., Eronen, M., Naurzbaev, M.M., 2008. Trends in recent temperature and radial tree growth spanning 2000 years across northwest Eurasia. Philos. Trans. R. Soc. Lond. Ser. B Biol. Sci. 363 (1501), 2271–2284. https://doi.org/10.1098/rstb.2007.2199.

Cao, J., Zhao, B., Gao, L., Li, J., Li, Z., Zhao, X.H., 2018. Increasing temperature sensitivity caused by climate warming, evidence from Northeastern China. Dendrochronologia 51, 101–111. https://doi.org/10.1016/j.dendro.2018.06.007.

Cao, J., Liu, H.Y., Zhao, B., Li, Z.S., Drew, D.M., Zhao, X.H., 2019. Species-specific and elevation-differentiated responses of tree growth to rapid warming in a mixed forest lead to a continuous growth enhancement in semi-humid Northeast Asia. For. Ecol. Manag. 448, 76–84. https://doi.org/10.1016/j.foreco.2019.05.065.

Charney, N.D., Babst, F., Poulter, B., Record, S., Trouet, V.M., Frank, D., Enquist, B.J., Evans, M.E.K., 2016. Observed forest sensitivity to climate implies large changes in 21st century North American forest growth. Ecol. Lett. 19 (9), 1119–1128. https://doi.org/10.1111/ele.12650.

Chen, X., Hu, B., Yu, R., 2005. Spatial and temporal variation of phenological growing season and climate change impacts in temperate eastern China. Global Change Biol. 11 (7), 1118–1130. https://doi.org/10.1111/j.1365-2486.2005.00974.x.

Cook, E.R., Kairiukstis, L.A., 1990. Methods of Dendrochronology: Applications in the Environmental Sciences. Kluwer Academic Publishers, Dordrecht, p. 390. https://doi.org/10.1007/978-94-015-7879-0.

D'Arrigo, R.D., Mashig, E., Frank, D.C., Wilson, R.J.S., Jacoby, G.C., 2005. Temperature variability over the past millennium inferred from Northwestern Alaska tree rings. Clim. Dynam. 24, 227–236. https://doi.org/10.1007/s00382-004-0502-1.

D'Arrigo, R., Wilson, R., Jacoby, G., 2006. On the long-term context for late twentieth century warming. J. Geophys. Res. 111, D03103. https://doi.org/10.1029/2005jd006352.

Delaygue, G., Bard, E., 2011. An Antarctic view of Beryllium-10 and solar activity for the past millennium. Clim. Dyn. 36 (11–12), 2201–2218. https://doi.org/10.1007/s00382-010-0795-1.

Deslauriers, A., Rossi, S., Anfodillo, T., Saracino, A., 2008. Cambial phenology, wood formation and temperature thresholds in two contrasting years at high altitude in southern Italy. Tree Physiol. 28 (6), 863–871. https://doi.org/10.1093/treephys/28.6.863.

Duan, J., Zhang, Q.B., 2014. A 449 year warm season temperature reconstruction in the southeastern Tibetan Plateau and its relation to solar activity. J. Geophys. Res. 119, 11578–11592. https://doi.org/10.1002/2014jd022422.

Dulamsuren, C., Hauck, M., Kopp, G., Ruff, M., Leuschner, C., 2017. European beech responds to climate change with growth decline at lower, and growth increase at higher elevations in the center of its distribution range (SW Germany). Trees (Berl.) 31 (2), 673–686. https://doi.org/10.1007/s00468-016-1499-x.

Esper, J., Cook, E.R., Schweingruber, F.H., 2002. Low-frequency signals in long tree-ring chronologies for reconstructing past temperature variability. Science 29 (5563), 2250–2252. https://doi.org/10.1126/science.1066208.

Esper, J., Krusic, P.J., Ljungqvist, F.C., Luterbacher, J., Carrer, M., Cook, E., Davi, N.K., Hartl-Meier, C., Kirdyanov, A., Konter, O., Myglan, V., Timonen, M., Treydte, K., Trouet, V., Villalba, R., Yang, B., Büntgen, U., 2016. Ranking of tree-ring based temperature reconstructions of the past millennium. Quat. Sci. Rev. 145, 134–151. https://doi.org/10.1016/j.quascirev.2016.05.009.

Fan, Z.X., Bräuning, A., Yang, B., Cao, K.F., 2009. Tree ring density-based summer temperature reconstruction for the central Hengduan Mountains in southern China. Global Planet. Change 65 (1–2), 1–11. https://doi.org/10.1016/j.gloplacha.2008.10.001.

Fritts, H.C., 1976. Tree Rings and Climate. Academic Press, New York, NY, USA.

Gray, L.J., Beer, J., Geller, M., Haigh, J.D., Lockwood, M., Matthes, K., Cubasch, U., Fleitmann, D., Harrison, G., Hood, L., Luterbacher, J., Meehl, G.A., Shindell, D., van Geel, B., White, W., 2010. Solar influence on climate. Rev. Geophys. 48 (4) https://doi.org/10.1029/2009RG000282.

Guo, B.D., Wang, X.C., Zhang, Y.D., 2019. Effects of accumulated and threshold temperatures on the radial growth of *Abies faxoniana* in the alpine timberline, Western Sichuan Plateau. Acta Ecol. Sin. 39 (3), 895–904 (in Chinese with English abstract).

Harsch, M.A., Hulme, P.E., Mcglone, M.S., Duncan, R.P., 2009. Are treelines advancing? A global meta-analysis of treeline response to climate warming. Ecol. Lett. 12 (10), 1040–1049. https://doi.org/10.1111/j.1461-0248.2009.01355.x.

He, M.H., Yang, B., Datsenko, N.M., 2014. A six hundred-year annual minimum temperature history for the central Tibetan Plateau derived from tree-ring width series. Clim. Dyn. 43 (3–4), 641–655. https://doi.org/10.1007/s00382-013-1882-x.

Hosoo, Y., Yoshida, M., Imai, T., Okuyama, T., 2002. Diurnal difference in the amount of immunogold-labeled glucomannans detected with field emission scanning electron microscopy at the innermost surface of developing secondary walls of differentiating conifer tracheids. Planta 215, 1006–1012. https://doi.org/10.2307/23387054.

Huang, J.G., Bergeron, Y., Zhai, L.H., Denneler, B., 2011. Variation in intra-annual radial growth (xylem formation) of *Picea mariana* (Pinaceae) along a latitudinal gradient in western Quebec, Canada. Am. J. Bot. 98, 792–800. https://doi.org/10.3732/ajb.1000074.

Huang, R., Zhu, H.F., Liang, E.Y., Liu, B., Shi, J.F., Zhang, R.B., Yuan, Y.J., Griessinger, J., 2019. A tree ring-based winter temperature reconstruction for the southeastern Tibetan Plateau since 1340 CE. Clim. Dyn. 53, 3221–3233. https://doi.org/10.1007/s00382-019-04695-3.

IPCC, 2013. In: Stocker, T.F., Qin, D., Plattner, G.K., Tignor, M., Allen, S.K., Boschung, J., Nauels, A., Xia, Y., Bex, V., Midgley, P.M. (Eds.), Climate Change 2013. The Physical Science Basis. Contribution of Working Group I to the Fifth Assessment Report of the Intergovernmental Panel on Climate Change. Cambridge University Press, Cambridge, UK and New York, NY, USA.

Jackson, D., 2009. Plant response to photoperiod. New Phytol. 181, 517–531. https://doi.org/10.1111/j.1469-8137.2008.02681.x.

Jeong, S.J., Chang-Hoi, H.O., Gim, H.J., Brown, M.E., 2011. Phenology shifts at start vs. end of growing season in temperate vegetation over the northern hemisphere for the period 1982–2008. Global Change Biol. 17 (7), 2385–2399. https://doi.org/10.1111/j.1365-2486.2011.02397.x.

Keeling, C.D., Chin, J.F.S., Whorf, T.P., 1996. Increased activity of northern vegetation inferred from atmospheric CO_2 measurements. Nature 382 (6587), 146–149. https://doi.org/10.1038/382146a0.

Keyimu, M., Li, Z.S., Zhang, G.S., Fan, Z.X., Wang, X.C., Fu, B.J., 2020. Tree ring–based minimum temperature reconstruction in the central Hengduan Mountains, China. Theor. Appl. Climatol. https://doi.org/10.1007/s00704-020-03169-5.

Körner, C., 2012. Alpine Treelines: Functional Ecology of the Global High Elevation Tree Limits. Springer Science Business Media, New York.

Kullman, L., 2013. Ecological tree line history and palaeoclimate – review of megafossil evidence from the Swedish Scandes. Boreas 42 (3), 555–567. https://doi.org/10.1111/bor.12003.

Li, Z.S., Zhang, Q.B., Ma, K., 2012. Tree-ring reconstruction of summer temperature for A.D. 1475–2003 in the central Hengduan Mountains, northwestern Yunnan, China. Climatic Change 110 (1–2), 455–467. https://doi.org/10.1007/s10584-011-0111-z.

Li, T., Li, J.B., 2017. A 564-year annual minimum temperature reconstruction for the east central Tibetan Plateau from tree rings. Global Planet. Change 157, 165–173. https://doi.org/10.1016/j.gloplacha.2017.08.018.

Liang, E.Y., Shao, X.M., Qin, N.S., 2008. Tree-ring based summer temperature reconstruction for the source region of the Yangtze River on the Tibetan Plateau. Glob. Planet Chagne. 61, 313–320. https://doi:10.1016/j.gloplacha.2007.10.008.

Liang, E.Y., Shao, X.M., Xu, Y., 2009. Tree-ring evidence of recent abnormal warming on the southeast Tibetan Plateau. Theor. Appl. Climatol. 98 (1), 9–18. https://doi.org/10.1007/s00704-008-0085-6.

Liang, E.Y., Leuschner, C., Dulamsuren, C., Wagner, B., Hauck, M., 2016a. Global warming-related tree growth decline and mortality on the north-eastern Tibetan Plateau. Climatic Change 134 (1), 163–176. https://doi.org/10.1007/s10584-015-1531-y.

Liang, H.X., Lyu, L.X., Wahab, M., 2016b. A 382-year reconstruction of august mean minimum temperature from tree-ring maximum latewood density on the southeastern Tibetan Plateau, China. Dendrochronologia 37, 1–8. https://doi.org/10.1016/j.dendro.2015.11.001.

Mann, M.E., Zhang, Z.H., Rutherford, S., Bradley, R.S., Hughes, M.K., Shindell, D., Ammann, C., Faluvegi, G., Ni, F., 2009. Global signatures and dynamical origins of the little ice age and medieval climate anomaly. Science 326 (5957), 1256–1260. https://doi.org/10.1126/science.1177303.

McMahon, M.J., Kofranek, A.M., Rubatzky, V.E., 2011. Plant Science: Growth, Development, and Utilization of Cultivated Plants, fifth ed. Prentince Hall, Boston.

Menzel, A., Sparks, T.H., Estrella, N., Koch, E., Aasa, A., Ahas, R., Alm-Kubler, K., Bissolli, P., Braslavska, O., Briede, A., 2006. European phonological response to climate change matches the warming pattern. Global Change Biol. 12, 1969–1976. https://doi.org/10.1111/j.1365-2486.2006.01193.x.

Mitchell, T.D., Jones, P.D., 2005. An improved method of constructing a database of monthly climate observations and associated high resolution grids. Int. J. Climatol. 25, 639–712. https://doi.org/10.1002/joc.1181.

Myneni, R.B., Keeling, C.D., Tucker, C.J., Asrar, G., Nemani, R.R., 1997. Increased plant growth in the northern high latitudes from 1981 to 1991. Nature 386 (6626), 698–702. https://doi.org/10.1038/386698a0.

Nemani, R.R., Keeling, C.D., Hashimoto, H., Jolly, W.N., Piper, S.C., Tucker, C.J., Myneni, R.B., Running, S.W., 2003. Climate-driven increases in global terrestrial net primary production from 1982 to 1999. Science 300 (5625), 1560–1563. https://doi.org/10.1126/science.1082750.

PAGES 2k Consortium, 2013. Continental-scale temperature variability during the past two millennia. Nat. Geosci. 6, 339–346. https://doi.org/10.1038/ngeo1797.

Pederson, N., Cook, E.R., Jacoby, G.C., Peteet, D.M., Griffin, K.L., 2004. The influence of winter temperatures on the annual radial growth of six northern range margin tree species. Dendrochronologia 22 (1), 7–29. https://doi.org/10.1016/j.dendro.2004.09.005.

Peng, C., Ma, Z., Lei, X., Zhu, Q., Chen, H., Wang, W.F., Liu, S.R., Li, W.Z., Fang, X.Q., Zhou, X.L., 2011. A drought-induced pervasive increase in tree mortality across Canada's boreal forests. Nat. Clim. Change 1, 467–471. https://doi.org/10.1038/nclimate1293.

Piao, S.L., Friedlingstein, P., Ciais, P., Viovy, N., Demarty, J., 2007. Growing season extension and its impact on terrestrial carbon cycle in the Northern Hemisphere over the past 2 decades. Global Biogeochem. Cycles 21, GB3018. https://doi.org/10.1029/2006GB002888.

Pumijumnong, N., Bräuning, A., Sano, M., Nakatsuka, T., Muangsong, C., Buajan, Supaporn, 2020. A 338-year tree-ring oxygen isotope record from Thai teak captures the variations in the Asian summer monsoon system. Sci. Rep. 10, 8966. https://doi.org/10.1038/s41598-020-66001-0.

Qi, Z.H., Liu, H.Y., Wu, X.C., Hao, Q., 2015. Climate-driven speedup of alpine treeline forest growth in the Tianshan Mountains, Northwestern China. Global Change Biol. 21 (2), 816–826. https://doi.org/10.1111/gcb.12703.

Reich, P.B., Oleksyn, J., 2008. Climate warming will reduce growth and survival of Scots pine except in the far north. Ecol. Lett. 11 (6), 588–597. https://doi.org/10.1111/j.1461-0248.2008.01172.x.

Roxy, M.K., Ritika, K., Terray, P., Murtugudde, R., Ashok, K., Goswami, B.N., 2015. Drying of Indian subcontinent by rapid Indian Ocean warming and a weakening land-sea thermal gradient. Nat. Commun. 6, 7423. https://doi.org/10.1038/ncomms8423.

Ryan, M.G., 2010. Temperature and tree growth. Tree Physiol. 30 (6), 667–668. https://doi.org/10.1093/treephys/tpq033.

Salzer, M.W., Hughes, M.K., Bunn, A.G., Kipfmueller, K.F., 2009. Recent unprecedented tree-ring growth in bristlecone pine at the highest elevations and possible causes. Proc. Natl. Acad. Sci. Unit. States Am. 106 (48), 20348–20353. https://doi.org/10.1073/pnas.0903029106.

Sano, M., Ramesh, R., Sheshshayee, M.S., Sukumar, R., 2012. Increasing aridity over the past 223 years in the Nepal Himalaya inferred from a tree-ring delta O-18 chronology. Holocene 22, 809–817. https://doi.org/10.1177/0959683611430338.

Schneider, L., Smerdon, J.E., Büntgen, U., Wilson, R.J.S., Myglan, V.S., Kirdyanov, A.V., Esper, J., 2015. Revising mid-latitude summer temperatures back to AD 600 based on a wood density network. Geophys. Res. Lett. 42, 4556–4562. https://doi.org/10.1002/2015GL063956.

Shi, C.M., Shen, M.G., Wu, X.C., Cheng, X., Li, X.Y., Fan, T.Y., Li, Z.S., Zhang, Y.D., Fan, Z.X., Shi, F.Z., Wu, G.C., 2019a. Growth response of alpine treeline forests to a warmer and drier climate on the southeastern Tibetan Plateau. Agric. For. Meteorol. 264, 73–79. https://doi.org/10.1016/j.agrformet.2018.10.002.

Shi, C.M., Sun, C., Wu, G.C., Wu, X.C., Chen, D.L., Masson-Delmotte, V., Li, J.P., Xue, J.Q., Li, Z.S., Ji, D.Y., Zhang, J., Fan, Z.X., Shen, M.G., Shu, L.F., Ciais, P., 2019b. Summer temperature over Tibetan Plateau modulated by Atlantic multidecadal variability. J. Clim. 32, 4055–4067. https://doi.org/10.1175/JCLI-D-17-0858.1.

Shi, C.M., Schneider, L., Hu, Y., Shen, M.G., Sun, C., Xia, J.Y., Forbes, B.C., Shi, P.L., Zhang, Y.D., Philippe, C., 2020. Warming-induced unprecedented high-elevation forest growth over the monsoonal Tibetan Plateau. Environ. Res. Lett. https://doi.org/10.1088/1748-9326/ab7b9b.

Shi, S.Y., Li, J.B., Shi, J.F., Zhao, Y.S., Huang, G., 2017. Three centuries of winter temperature change on the southeastern Tibetan plateau and its relationship with the Atlantic Multidecadal Oscillation. Clim. Dynam. 49, 1305–1319. https://doi.org/10.1007/s00382-016-3381-3.

Schweingruber, F., 2007. Wood Structure and Environment https:/doi.org/10.1007/978-3-540-48548-3.

Stoffel, M., Khodri, M., Corona, C., Guillet, S., Poulain, V., Bekki, S., Guiot, J., Luckman, B.H., Oppenheimer, C., Lebas, N., Beniston, M., Masson-Delmotte, V., 2015. Estimates of volcanic-induced cooling in the Northern Hemisphere over the past 1500 years. Nat. Geosci. 8, 784–788. https://doi.org/10.1038/ngeo2526.

Voelker, S.L., Brooks, J.R., Meinzer, F.C., Anderson, R., Bader, K.F., Battipaglia, G., Becklin, K.M., Beerling, D., Bert, D., Betancourt, J.L., Dawson, T.E., Domec, J.C., Guyette, R.P., Koerner, C., Leavitt, S.W., Linder, S., Marshall, J.D., Mildner, M., Ogee, J., Panyushkina, I., Plumton, H.J., Pregitzer, K., Saurer, M., Smith, A.R., Siegwolf, R.W., Stambaugh, M.C., Talhelm, A.F., Tardif, J.C., Van de Water, P.K., Ward, J.K., Wingate, L., 2016. A dynamic leaf gas-exchange strategy is conserved in woody plants under changing ambient CO_2: evidence from carbon isotope discrimination in paleo and CO_2 enrichment studies. Global Change Biol. 22 (2), 889–902. https://doi.org/10.1111/gcb.13102.

Wang, J.L., Yang, B., Qin, C., Kang, S.Y., He, M.H., Wang, Z.Y., 2014. Tree-ring inferred annual mean temperature variations on the southeastern Tibetan Plateau during the last millennium and their relationships with the Atlantic Multidecadal Oscillation. Clim. Dyn. 43, 627–640. https://doi.org/10.1007/s00382-013-1802-0.

Wang, J.L., Yang, B., Ljungqvist, F.C., 2015. A millennial summer temperature reconstruction for the eastern Tibetan Plateau from tree-ring width. J. Clim. 28 (13), 5289–5304. https://doi.org/10.1175/JCLI-D-14-00738.1.

Wang, J.L., Yang, B., Ljungqvist, F.C., Luterbacher, J., Osborn, T.J., Briffa, K.R., Zorita, E., 2017a. Internal and external forcing of multidecadal Atlantic climate variability over the past 1200 years. Nat. Geosci. 10, 512–518. https://doi.org/10.1038/NGEO2962.

Wang, Q., Zhang, T.B., Yi, G.H., Chen, T.T., Bie, X.J., He, Y.X., 2017b. Tempo-spatial variations and driving factors analysis of net primary productivity in the Hengduan Mountain area from 2004 to 2014. Acta Ecol. Sin. 37 (9), 3084–3095 (in Chinese with English abstract).

Way, D.A., Oren, R., 2010. Differential responses to changes in growth temperature between trees from different functional groups and biomes: a review and synthesis of data. Tree Physiol. 30, 669–688. https://doi.org/10.1093/treephys/tpq015.

Wigley, T.M.L., Briffa, K.R., Jones, P.D., 1984. On the average of correlated time series, with applications in dendroclimatology and hydrometeorology. J. Clim. Appl. Meteorol. 23, 201–213 https://doi.org/10.1175/1520-0450(1984)023<0201:OTAVOC>2.0.CO;2.

Williams, A.P., Allen, C.D., Millar, C.I., Swetnam, T.W., Michaelsen, J., Still, C.J., 2010a. Forest responses to increasing aridity and warmth in the southwestern United States. Proc. Natl. Acad. Sci. U. S. A 107 (50), 21289–21294. https://doi.org/10.1073/pnas.0914211107.

Williams, A.P., Michaelsen, J., Leavitt, S.W., Still, C.J., 2010b. Using tree rings to predict the response of tree growth to climate change in the continental United States during the twenty-first century. Earth Interact. 14 (19), 256–261. https://doi.org/10.1175/2010EI362.1.

Williams, A.P., Xu, C.G., Mcdowell, N.G., 2011. Who is the new sheriff in town regulating boreal forest growth? Environ. Res. Lett. 6 (4), 526–533. https://doi.org/10.1088/1748-9326/6/4/041004.

Williams, C.M., Henry, H.A., Sinclair, B.J., 2015. Cold truths: how winter drives responses of terrestrial organisms to climate change. Biol. Rev. 90 (1), 214–235. https://doi.org/10.1111/brv.12105.

Wilson, R.J.S., Luckman, B.H., 2002. Tree-ring reconstruction of maximum and minimum temperatures and the diurnal temperature range in British Columbia. Canada. Dendrochronologia 20 (3), 257–268. https://doi.org/10.1078/1125-7865-00023.

Wilson, R.J.S., Luckman, B.H., 2003. Dendroclimatic reconstruction of maximum summer temperatures from upper treeline sites in Interior British Columbia, Canada. Holocene 13, 851–861. https://doi.org/10.1191/0959683603hl663rp.

Wilson, R., Anchukaitis, K., Briffa, K.R., Büntgen, U., Cook, E., D'Arrigo, R., Davi, N., Esper, J., Frank, D., Gunnarson, B., Hegerl, G., Helama, S., Klesse, S., Krusic, P.J., Linderholm, H.W., Myglan, V., Osborn, T.J., Rydval, M., Schneider, L., Schurer, A., Wiles, G., Zhang, P., Zorita, E., 2016. Last millennium northern hemisphere summer temperatures from tree rings: Part I: the long term context. Quat. Sci. Rev. 134, 1–18. https://doi.org/10.1016/j.quascirev.2015.12.005.

Yang, B., Qin, C., Wang, J.L., He, M.H., Melvin, T.M., Osborn, T.J., Briffa, K.R., 2014. A 3500-year tree-ring record of annual precipitation on the northeastern Tibetan Plateau. Proc. Natl. Acad. Sci. U. S. A 111 (8), 2903–2908. www.pnas.org/cgi/doi/10.1073/pnas.1319238111.

Zhang, Q.B., Cheng, G.D., Yao, T.D., Kang, X.C., Huang, J.G., 2003. A 2326-year tree-ring record of climate variability on the northeastern Qinghai-Tibetan Plateau. Geophys. Res. Lett. 30 (14), 1739–1742. https://doi.org/10.1029/2003GL017425.

Zhu, L.J., Zhang, Y.D., Li, Z.S., Guo, B.D., Wang, X.C., 2016b. A 368-year maximum temperature reconstruction based on tree-ring data in the northwestern Sichuan Plateau (NWSP), China. Clim. Past 12 (7), 1485–1498. https://doi.org/10.5194/cp-12-1485-2016.